

We SRS2 11

Adaptive Least-squares RTM for Subsalt Imaging

C. Zeng (TGS), S. Dong (TGS), B. Wang (TGS) & Z. Zhang* (TGS)

SUMMARY

We propose an adaptive solution for subsalt imaging using least-squares reverse time migration (LSRTM). We aim to address the typical problems in subsalt imaging such as minor velocity errors and salt related migration artefacts. We first demonstrate the modelling based noise cancellation capability of LSRTM with the field data from the Gulf of Mexico (GoM). LSRTM distinctly enhances signals and removes migration artefacts even when their characteristics are similar on seismic images. We also propose a crosscorrelation based confidence level to control the quality of data matching. The application on the GoM field data shows improved termination of sediments toward salt boundaries in the shadow zone. The strong salt halo artefacts are also suppressed effectively after the adaptive LSRTM updating.

Introduction

Recently inversion-based imaging algorithms (Schuster, 1993, Nemeth et al., 1999, Duquet et al., 2000) such as least-squares reverse time migration (LSRTM) have gained a lot of attention of the geophysicists (e.g., Tang, 2009, Wong et al., 2011, and Dai et al., 2013). Different from conventional migration algorithms based on the imaging condition, LSRTM uses geophysical inversion to iteratively refine the seismic image toward true reflectivity (Dong et al., 2012) and overcomes many of the shortcomings of conventional migration methods. Previous studies including field data tests (e.g., Zeng et al., 2014a, and Zhang et al., 2015) show that LSRTM can reduce migration artefacts, balance image amplitudes, reveal weak signal, and improve the image coherency. These advantages make LSRTM very attractive for subsalt imaging.

For subsalt imaging, we have to address many practical issues (Wang et al., 2013) to bring LSRTM from synthetic testing to field production. One major problem is that the original theory of LSRTM requires a perfect migration velocity or the least-squares fitting between field data and modelled data will be erroneous. Unfortunately, velocity errors always exist in the real world and it seems unattainable to make the short wavelength velocity components accurate enough near the salt (Etgen et al., 2014). The data mismatch produces extra artefacts in the data residual then contaminates the image updating. Particularly, large errors can occur at far offsets and late arrivals corresponding to subsalt reflections and cause a convergence problem in subsalt areas. On the other side, subsalt images often suffer from strong salt-related migration artefacts. A typical artefact is a type of noise that is parallel to the salt flank or base of salt (BOS), known as a salt “halo” that strongly degrades the image near the salt.

To address the above subsalt imaging problems, we first investigate the modelling-based noise cancellation capability of LSRTM using field data from the Gulf of Mexico (GoM). Then we propose a quality controlled adaptive solution for LSRTM so that it can tolerate minor velocity errors and converge fast in subsalt by automatic suppression of the halo artefacts. We finally apply this adaptive strategy to the GoM field data to demonstrate the practical effectiveness.

Modelling Based Noise Cancellation

An important feature of LSRTM is that it can iteratively remove the migration artefacts without hurting the effective signal on seismic images. When imaging complex subsalt structures, we often see undesired migration swing artefacts due to uneven illumination or insufficient data coverage. In many cases, the artefacts share the same characteristics with the true signal such as similar dips. This causes difficulties in differentiating the artefacts and true geologic events in the image domain and introduces challenges to remove the noise using conventional postmigration processing methods. Figure 1a illustrates the problem with a conventional RTM image migrated from a set of wide-azimuth (WAZ) data from the GoM. Strong migration swings appear in the area near the salt boundary. On the left side of the image (the faulting zone), the fault planes have similar dip and geometric pattern to the right side swing noise. A conventional postprocessing routine (e.g., F-K filtering) can remove the steeply dipping migration swings but it will also wipe out the fault planes on the same image.

To overcome this problem, we use LSRTM to cancel the swing noise and enhance the fault plane simultaneously. After LSRTM modelling, the true geologic features on the image create events on the time-domain synthetic data that are consistent with those in the field data. While the artefacts create spurious events that do not physically exist in the field data. This generates polarity-reversed “artefacts” on the time-domain residual and phase-reversed depth-domain events after the subsequent remigration for gradient computation. Figure 1b demonstrates the gradient of LSRTM during the first iteration. By observing the wiggles of the gradient, we find that in the faulting zone the RTM image and the LSRTM gradient have same polarity, while in the area containing strong migration swings, the polarity of the artefacts are reversed compared to those on the original RTM image. Thus a

summation (Figure 1c) of the RTM image and the gradient will cancel the out-of-phase swings but enhance the in-phase fault planes and sediments.

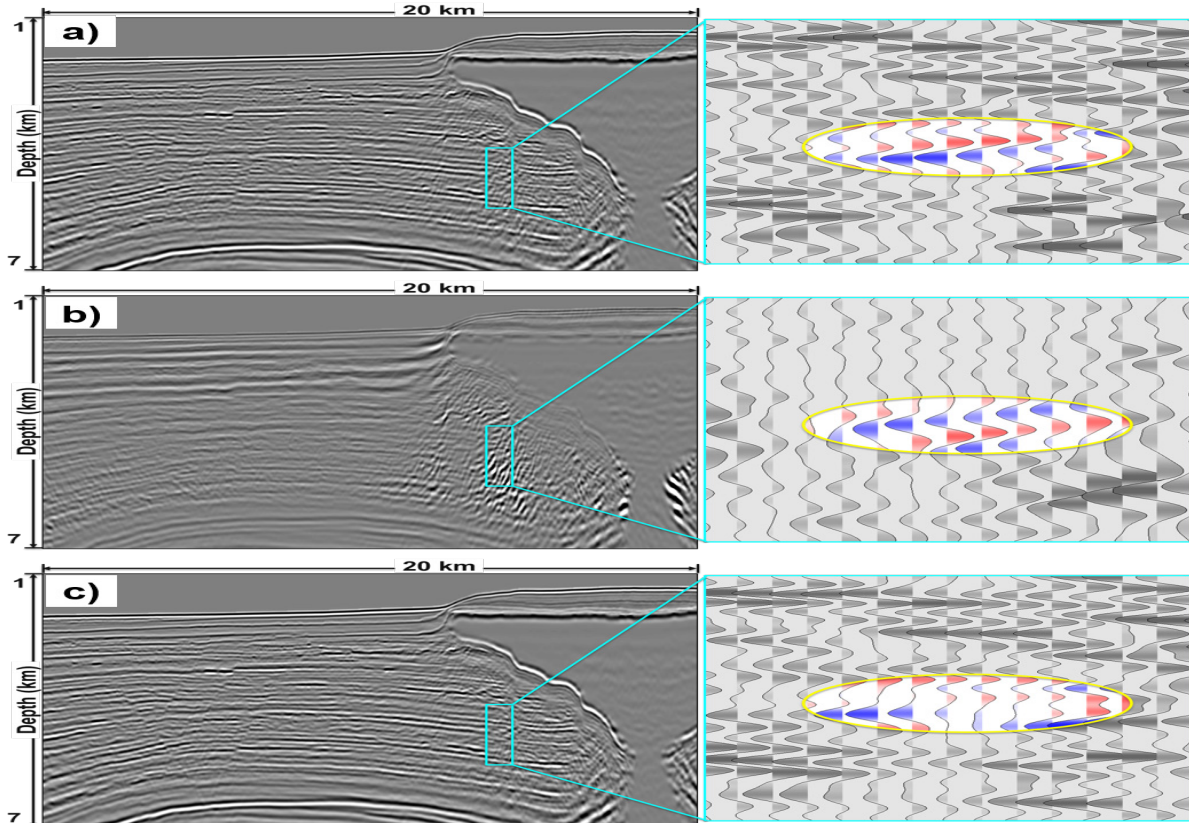


Figure 1 a) Conventional RTM image, b) LSRTM gradient of the first iteration, c) LSRTM image after updating. The steeply dipping fault planes are enhanced while the swing artefacts (zoomed on the right side) are cancelled out regardless of their similar dipping and geometric pattern.

Quality Controlled Adaptive Data Fitting

The quality of LSRTM image highly relies on the accuracy of the velocity model. Any error in the velocity will propagate into the inversion and will be amplified during the iterations. In theory, LSRTM requires perfect migration velocity to ensure the convergence. However, for real-world subsalt imaging, velocity errors are unavoidable. This introduces unwanted time shifts in synthetic waveforms with respect to the field data. To make LSRTM tolerable to minor velocity errors, Luo and Hale (2014) proposed to use dynamic warping (Hale, 2013) to modify the arrival time of the field data and force them to align with the synthetic data. For LSRTM this data domain adjustment is feasible because it is done only once before the first iteration and imposes no extra computation cost for the inversion. Since the modelling and migration kernels share the same velocity model, the synthetic data are self-consistent with the migrated image in terms of time-to-depth mapping.

For quality control of the dynamic warping, we introduce a confidence level to measure the reliability of the warped data to evaluate the quality of the data adaptive correction. The confidence level at each sample point is calculated by a 2D normalized crosscorrelation as follows:

$$c_i = \frac{\sum_{ix=-h}^h \sum_{it=-l}^l (d_i - \bar{d})(u_i - \bar{u})}{\sqrt{\sum_{ix=-h}^h \sum_{it=-l}^l (d_i - \bar{d})^2} \sqrt{\sum_{ix=-h}^h \sum_{it=-l}^l (u_i - \bar{u})^2}} \quad (1)$$

where d and u are the warped input and synthetic samples, respectively. The h and l correspond to the half window size along the spatial and temporal direction. Figure 2 shows an example of the confidence level computed for dynamic warping the input and modelled shot gather.

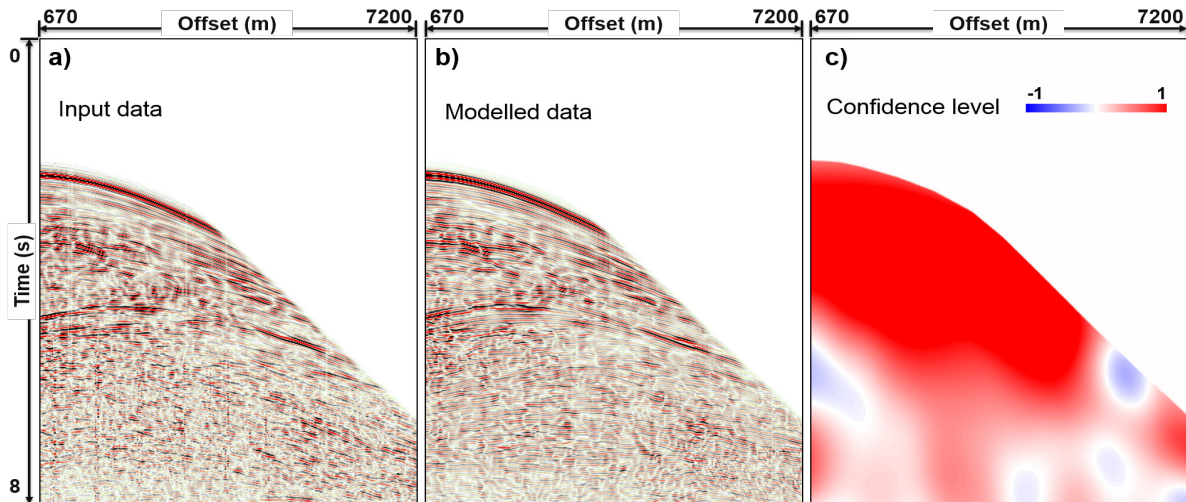


Figure 2 a) Input shot record, b) Synthetic shot record, and c) the confidence level for residual weighting based on crosscorrelation.

GoM Field Data Applications

The success of the adaptive LSRTM for subsalt imaging is confirmed by its application to Patriot 3D WAZ data based in the GoM. Detailed image improvements after the adaptive LSRTM are illustrated in a typical inline section shown in Figure 3. The middle part of the conventional RTM section (Figure 3a) contains significant migration swings. In the shadow area near the salt flank, strong low-frequency halo artefacts occur along the overturned salt boundary. By applying the adaptive LSRTM, the middle part of the image (Figure 3b) is more coherent due to the cancellation of the swing noise. In addition, the terminations of the sediments against the salt boundary are significantly improved because of the suppression of the salt halo artefacts.

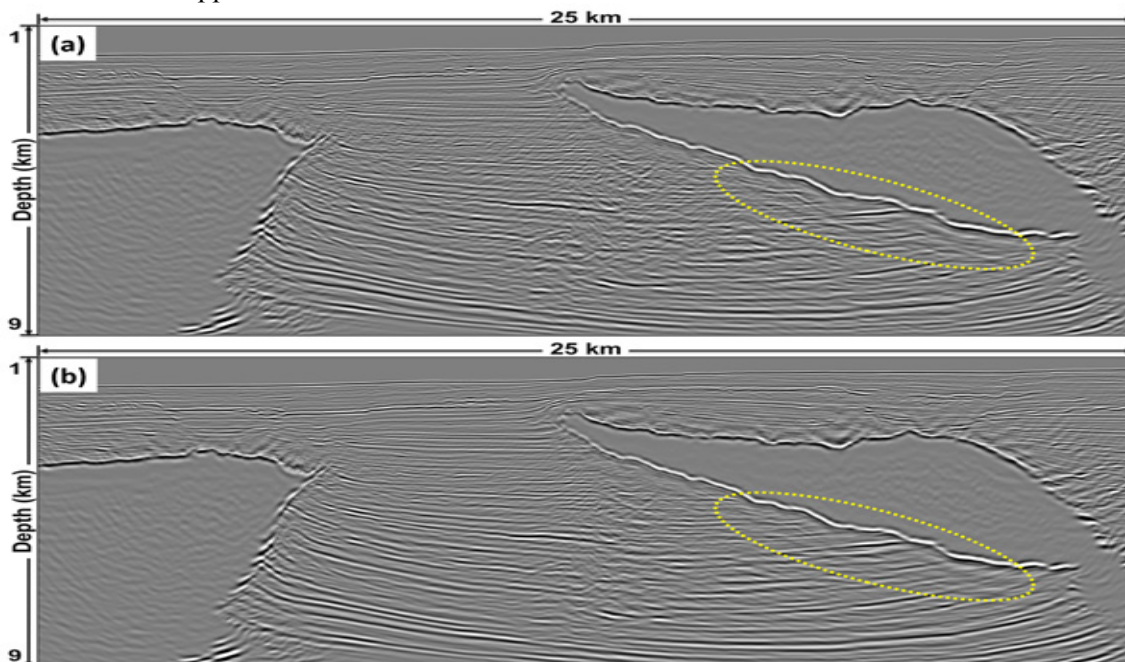


Figure 3 Inline section of the (a) conventional RTM image and (b) adaptive LSRTM image migrated from the Patriot 3D WAZ data. The shadow area is marked by the dotted ellipse.

Conclusions

We present a quality-controlled adaptive approach to LSRTM, focusing on subsalt imaging. The adaptive LSRTM overcomes the practical issues such as minor velocity errors and strong salt-related “halo” artefacts. The GoM field data experiments show significant improvements for images near the steeply dipping salt flanks and those below the base of salt.

Acknowledgements

The authors highly appreciate Jean Ji for the data preparation, Zhigang Zhang, and Sang Suh for the GPU programming, and Connie VanSchuyver for the manuscript proofreading. They are grateful to Zhaohong Wu, Darrell Armentrout, Li Li, and Taejong Kim for their great efforts on field data testing. They also thank Gary Rodriguez, Henrik Roende, and Zhiming Li for continuous support as well as the TGS management for permission to publish. The GoM field data are courtesy of TGS and WesternGeco LLC.

References

- Dai, W., Huang, Y., and Schuster, G.T. [2013] Least-squares reverse time migration of marine data with frequency-selection encoding. *Geophysics*, **78**(4), S233-S242.
- Dong, S., Cai, J., Guo, M., Suh, S., Zhang, Z., Wang, B. and Li, Z. [2012] Least-squares reverse time migration: towards true amplitude imaging and improving the resolution. *82nd Annual International Meeting, SEG*, Expanded Abstracts.
- Duquet, B., Marfurt, K.J. and Dellinger, J.A. [2000] Kirchhoff modeling, inversion for reflectivity, and subsurface illumination. *Geophysics*, **65**(4), 1195-1209.
- Etgen, J.T., Ahmed, I., Zhou, M. [2014] Seismic adaptive optics. *84th Annual International Meeting, SEG*, Expanded Abstracts, 4411-4415.
- Hale, D., 2013, Dynamic warping of seismic images. *Geophysics*, **78**(2), S105-S115.
- Luo, S. and Hale, D. [2014] Least-squares migration in the presence of velocity errors. *Geophysics*, **79**(4), S153-S161.
- Nemeth, T., Wu, C. and Schuster, G.T. [1999] Least-squares migration of incomplete reflection data. *Geophysics*, **64**(1), 208-221.
- Schuster, G.T. [1993] Least-squares cross-well migration. *63rd Annual International Meeting, SEG*, Expanded Abstracts, 110–113.
- Tang, Y. [2009] Target-oriented wave-equation least-squares migration/inversion with phase-encoded Hessian. *Geophysics*, **74**(6), WCA95-WCA104.
- Wang, B., Dong, S., and Suh, S. [2013] Practical aspects of least-squares reverse time migration. *75th Conference and Exhibition, EAGE*, Extended Abstracts, We P09 02.
- Wong, M., Ronen, S., and Biondi, B. [2011] Least-squares reverse-time migration/inversion for ocean bottom data: A case study. *81st Annual International Meeting, SEG*, Expanded Abstracts, 2369-2373.
- Zeng, C., Dong, S., and Wang, B. [2014a] Least-squares reverse time migration: inversion-based imaging toward true reflectivity. *The Leading Edge*, **33**(9), 962-968.
- Zeng, C., Dong, S., Mao, J., and Wang, B. [2014b] Broadband least-squares reverse time migration for complex structure imaging. *84th Annual International Meeting, SEG*, Expanded Abstracts, 3715-3719.
- Zhang, Y., Duan, L., and Xie, Y. [2015] A stable and practical implementation of least-squares reverse time migration. *Geophysics*, **80**(1), V23-V31.